



## **Optical techniques as validation tools for finite element modeling of biomechanical structures, demonstrated in bird ear research**

Pieter Muyshondt, Daniël De Greef, Joris Soons, and Joris J. J. Dirckx

Citation: [AIP Conference Proceedings](#) **1600**, 330 (2014); doi: 10.1063/1.4879599

View online: <http://dx.doi.org/10.1063/1.4879599>

View Table of Contents: <http://scitation.aip.org/content/aip/proceeding/aipcp/1600?ver=pdfcov>

Published by the [AIP Publishing](#)

---

### **Articles you may be interested in**

[Experimentally validated finite element model of electrocaloric multilayer ceramic structures](#)

J. Appl. Phys. **116**, 044511 (2014); 10.1063/1.4891298

[A detailed biomechanical finite element tongue model](#)

J. Acoust. Soc. Am. **123**, 3080 (2008); 10.1121/1.2932886

[Comparison of finite element model of scattering with experimental results from the Experimental Validation of Acoustic modeling techniques \(EVA\) sea test](#)

J. Acoust. Soc. Am. **122**, 2974 (2007); 10.1121/1.2942610

[An approach to finite-element modeling of the middle ear](#)

J. Acoust. Soc. Am. **85**, S67 (1989); 10.1121/1.2027094

[Finite-element modeling of the middle-ear ossicles](#)

J. Acoust. Soc. Am. **69**, S14 (1981); 10.1121/1.386393

---

# Optical techniques as validation tools for finite element modeling of biomechanical structures, demonstrated in bird ear research

Pieter Muyshondt<sup>a</sup>, Daniël De Greef<sup>a</sup>, Joris Soons<sup>a</sup>, Joris J. J. Dirckx<sup>a</sup>

<sup>a</sup> *University of Antwerp, Laboratory of BioMedical Physics, Groenenborgerlaan 171, B-2020 Antwerp, Belgium*

**Abstract.** In this paper we demonstrate the potential of stroboscopic digital holography and laser vibrometry as tools to gather vibration data and validate modelling results in complex biomechanical systems, in this case the avian middle ear. Whereas the middle ear of all mammal species contains three ossicles, birds only feature one ossicle, the columella. Despite this far simpler design, the hearing range of most birds is comparable to mammals, and is adapted to operate under very diverse atmospheric circumstances. This makes the investigation of the avian middle ear potentially very meaningful, since it could provide knowledge that can improve the design of prosthetic ossicle replacements in humans such as a TORP (Total Ossicle Replacement Prosthesis).

In order to better understand the mechanics of the bird's hearing, we developed a finite element model that simulates the transmission of an incident acoustic wave on the eardrum via the middle ear structures to the fluid of the inner ear. The model is based on geometry extracted from stained  $\mu$ CT data and is validated using results from stroboscopic digital holography measurements on the eardrum and LDV measurements on the columella footplate. This technique uses very short high-power laser pulses that are synchronized to the membrane's vibration phase to measure the dynamic response of the bird's eardrum to an incident acoustic stimulus. Vibration magnitude as well as phase relative to the sound wave can be deduced from the results, the latter being of great importance in the elastic characterization of the tympanic membrane.

In this work, the setup and results from the optical measurements, as well as the properties and optimization of the finite element model are presented. Observed phase variations across the eardrum's surface on the holography results strongly suggest the presence of internal energy losses in the membrane due to damping. Therefore, a viscoelastic characterisation of the model based on a complex modulus with a loss factor is chosen. Optimal values for a number of essential material parameters are determined by applying inverse analysis techniques using the experimental results. The result is a realistic dynamic model of the avian middle ear that will be used in the future to enhance treatment of middle ear pathologies in humans.

## 1. INTRODUCTION

Optical interferometry has become a prominent technique in studies on biomechanical systems, because of its high sensitivity and non-contact nature. Digital stroboscopic holography is an ideal full-field method to measure vibrations on membranes, and is therefore a complimentary tool to laser Doppler vibrometry (LDV) in the study of biomechanical vibrations. We demonstrate the combination of these two methods in a specific application example of the avian middle ear.

The avian middle ear is a peculiar biomechanical system that serves as an impedance match between incoming sound waves in air and acoustic waves in the inner ear fluid. In contrast to the mammal middle ear, which contains three ossicles and a number of muscles and ligaments, the avian middle ear contains only one ossicle, the columella, one ligament and one muscle. Despite this far simpler design, birds are able to perceive sound signals in a frequency range that is comparable to mammals [1]. Despite these interesting properties, the avian middle ear has not been given the same research attention as the mammal middle ear.

This paper presents the current state of our research of avian middle ear mechanics through stroboscopic digital holography, LDV and finite element modelling. The model's geometry is deduced from  $\mu$ CT measurements and its parameters are optimized using the experimental results. The work will provide novel insights in the functioning of this mechanically simpler variant to mammal middle ears, and therefore have important consequences in the development of middle ear ossicular replacement prostheses. Because some of the current middle ear prostheses designs (such as a TORP - Total Ossicle Replacement Prosthesis) qualitatively resemble the avian middle ear,

studying this system will assist in determining the optimal shape, parameters, material choice and placement of these prostheses.

## 2. METHOD

### 2.1 Stroboscopic Digital Holography and LDV Setup

In stroboscopic digital holography, very short pulses are synchronized to the phase of a vibrating object, so that the full-field displacement map of the object's surface at the chosen phase can be calculated after combining it with a reference hologram of the object in rest. By cycling these pulses stepwise through the vibration period, the entire time-resolved motion the surface is obtained. Figure 1 shows our setup that was developed to measure the dynamic displacement of the duck tympanic membrane (TM). The sample was placed behind an acoustic stimulation element (ASE), which controls and monitors the acoustic stimulus. Thanks to the very short high-energy pulses from the laser, sound-induced vibrations at both quasi-static and acoustic frequencies are measurable. More details on the setup can be found in [2] and a dedicated paper will be published soon by the second author of this text.

A segment of the left half of a Mallard duck (*Anas platyrhynchos*) containing the middle ear was dissected from a decapitated animal and the ear canal was drilled away. This was necessary to illuminate the full surface of the TM perpendicularly and thereby align the setup's sensitivity vector with the expected main vibration direction of the TM, i.e. out-of-plane. To increase the naturally low light reflectivity of the TM without influencing the vibrational behavior, the membrane was painted with a thin layer of a 5% TiO<sub>2</sub> suspension in deionized water. During the entire preparation, the sample was kept moist by use of a humidifier (Bionaire) in order to minimize fast dehydration effects and subsequent change of elastic parameters.

In order to make a better assessment of the transfer function of the entire middle ear system, the full-field stroboscopic holography measurements on the TM were complemented with single-point LDV measurements at the center of the footplate of the columella. This is the final structure of the middle ear and induces pressure waves in the inner ear fluid. These measurements were performed on another animal than the holography measurements. In order to get visual access to the medial surface of the footplate, the cochlea of the inner ear needed to be drilled away. No further reflectivity enhancements were necessary to acquire a sufficient response signal, as demonstrated by the results on a fresh sample. For these measurements as well, the input stimulation was an acoustic signal presented to the lateral side of the TM through a rigid tube. The sound pressure level was monitored by a probe microphone, with its tip located inside the tube and close to entrance of the shallow ear canal.

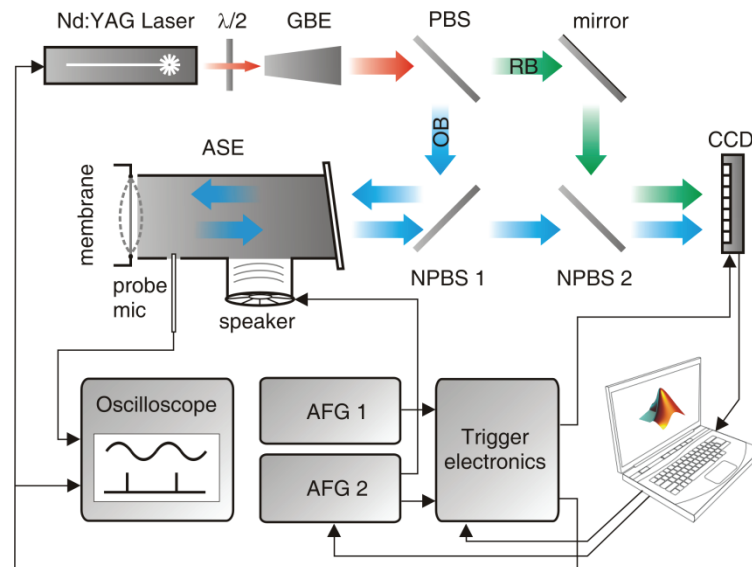


**FIGURE 1.** Overview of the setup for digital holography. GBE: Galilean beam expander, (N)PBS: (Non-)polarizing beamsplitter, OB: Object beam, RB: Reference beam, ASE: Acoustic stimulation element, AFG: Arbitrary function generator.

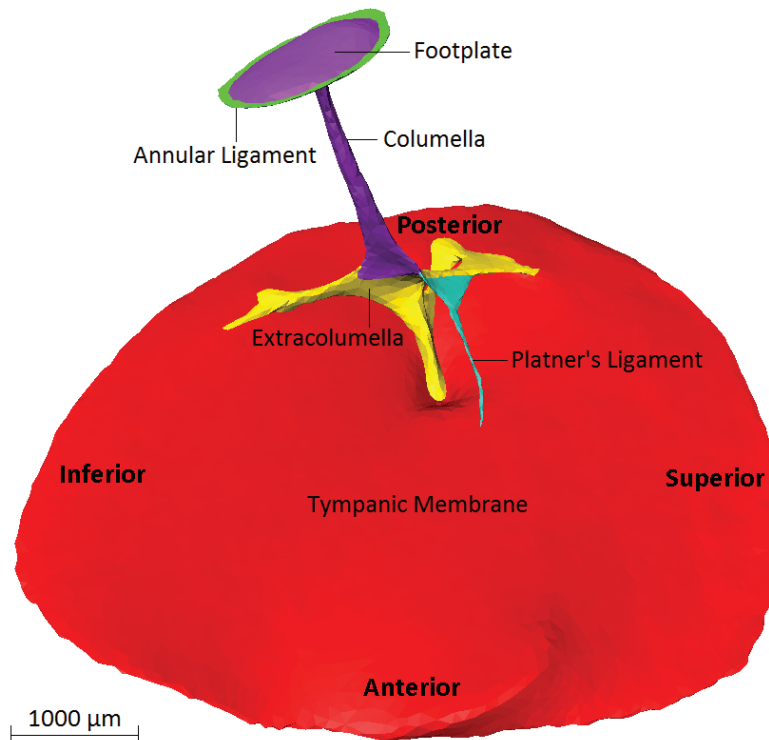


**FIGURE 2.** Geometrical surface model of the middle ear of a mallard duck, reconstructed from  $\mu$ CT measurements. The different components and anatomical orientations are indicated.

## 2.2 Finite Element Model

Geometrical data were obtained from  $\mu$ CT measurements performed at UGCT, UGhent [3] on a segment of the left skull half of a dead mallard duck (other animal than in optical measurements). In order to enhance the X-ray contrast of different types of soft tissue, the sample was stained in a daily refreshed 2,5% PTA (Phosphotungstic acid) solution in deionized water for 48 hours before the scan. From these data, different middle ear structures were segmented using Amira (Visage Imaging) to create a surface model of the middle ear which is needed to create a realistic finite element model.

Within the surface model, as depicted on Fig. 2, five different structures could be distinguished: the tympanic membrane, Platner's ligament, the cartilaginous extracolumella and the bony columella with a footplate bounded by an annular ligament. Other ligaments mentioned in literature were not observed and therefore not considered in the geometry. The final geometrical surface model, consisting of 15 000 triangle-shaped faces after simplification and smoothing of the surface, was exported as an STL-file that could be imported in finite element software (COMSOL Multiphysics 4.3b, The Structural Mechanics Module) in order to create a mechanical model.

Finite element studies of the human middle ear have indicated that a viscoelastic characterization of the soft tissue structures is necessary to predict the observed behavior [4]. Therefore, we chose to introduce a complex elastic modulus with an isotropic loss factor. Since there are no literature values available for the elastic parameters of the avian middle ear, human and other viscoelastic material parameters were used as initial values instead. As explained in the next section, some of these parameters will be optimized using the experimental data. In table (1) starting values for different parameters of all components are listed. All parameters are isotropic.

**TABLE (1).** Starting material parameters used in the current finite element model. All mass densities and Poissons are taken from [5]; Values indicated with <sup>a</sup> also taken from [5]; <sup>b</sup> taken from [6]; <sup>c</sup> taken from [7]; <sup>d</sup> taken from [4]; <sup>e</sup> taken from [8].

Component	Mass density [ $10^3 \text{ kg/m}^3$ ]	Young's modulus [MPa]	Loss factor	Poisson's ratio
TM	1.2	20 <sup>a</sup>	0.078 <sup>d</sup>	0.3
Columella	2.2	1410 <sup>a</sup>	0 <sup>e</sup>	0.3
Extracolumella	1.2	39.2 <sup>b</sup>	0.078 <sup>d</sup>	0.3
Platner's Ligament	1.2	21 <sup>c</sup>	0.078 <sup>d</sup>	0.3
Annular Ligament	1.2	0.0412 <sup>a</sup>	0.078 <sup>d</sup>	0.3

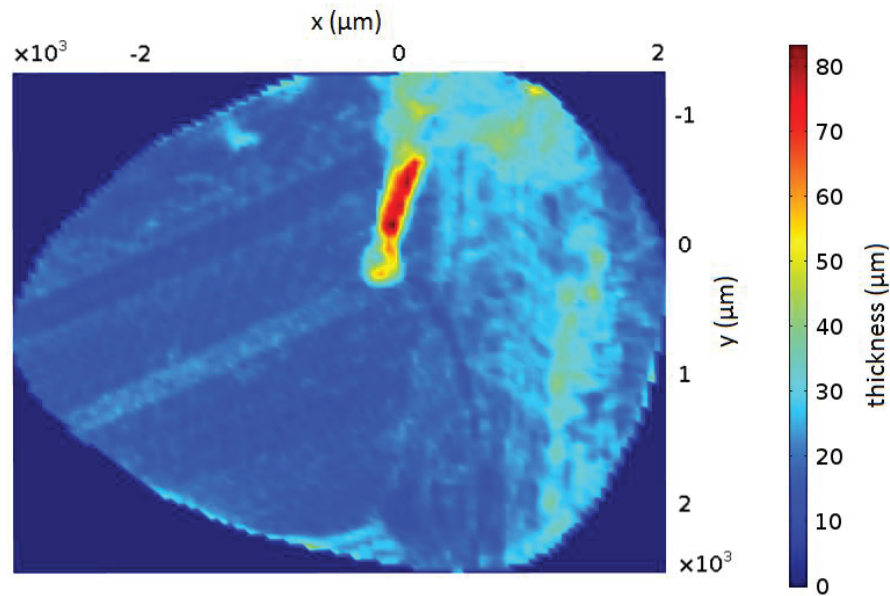


**FIGURE 3.** Geometrical surface model of the middle ear of a mallard duck, reconstructed from  $\mu$ CT measurements. The different components and anatomical orientations are indicated.

The finite element model was built up by two types of mesh elements: 2D triangle-shaped shell elements for the tympanic membrane, which are appropriate for thin structures, and 3D tetrahedral solid elements for the remaining middle ear components. Because shell elements are only two-dimensional, one needs a procedure to account for the finite and variable thickness of the tympanic membrane. This was realized by defining a function on the eardrum elements that interpolates the thickness distribution obtained from the original image segmentation data, as shown on Fig. 2. Despite the two-dimensional mathematical framework of shell elements, they still account for typical three-dimensional properties like bending stiffness and inertia.

To model the incident acoustic waves at the tympanic membrane, a uniform harmonic load of 1 Pa was applied at the outer (i.e. lateral) surface of the eardrum. The presence of the cochlea in the inner ear behind the columella footplate was simulated by a viscoelastic spring foundation that was introduced at the footplate to account for the impedance caused by the cochlear fluid.

The tympanic membrane was fully constrained at the edge, as well as the annular ligament and the end of the Platner's ligament. To determine the linear response from the middle ear to harmonic loads, the computations were performed in the frequency domain. From these calculations the resulting displacement magnitude and phase over the entire eardrum were deduced.

### 2.3 Optimization of the Model

As mentioned before, there are no avian middle ear properties available in literature. Therefore, the mechanical parameters of the middle ear components were validated by performing an inverse analysis routine in which the finite element model is compared with holography measurements. In this procedure the aim is to optimize the model in a certain way so that it approximates the experiment as well as possible. Therefore, an intelligently defined object function is to be minimized. The object function that was minimized in this work is defined as

$$\chi^2(p) = \sum_{i=1}^n \left[ \left( M_{\text{mod}}(r_i, p) - M_{\text{exp}}(r_i) \right)^2 + \left( \phi_{\text{mod}}(r_i, p) - \phi_{\text{exp}}(r_i) \right)^2 \right]. \quad (1)$$

In this equation the summation index  $i$  runs over the number of evaluated points  $n$  on the eardrum surface. The  $r_i$  represent the spatial coordinates on the eardrum and  $p$  is the set of model parameters to be optimized.  $M$  represents the magnitude normalized to 1 and  $\phi$  the vibration phase. The subscripts 'mod' and 'exp' denote model and experimental results, respectively. Magnitude maps were normalized to their respective maximal magnitude to prevent erroneously large values for the object function.

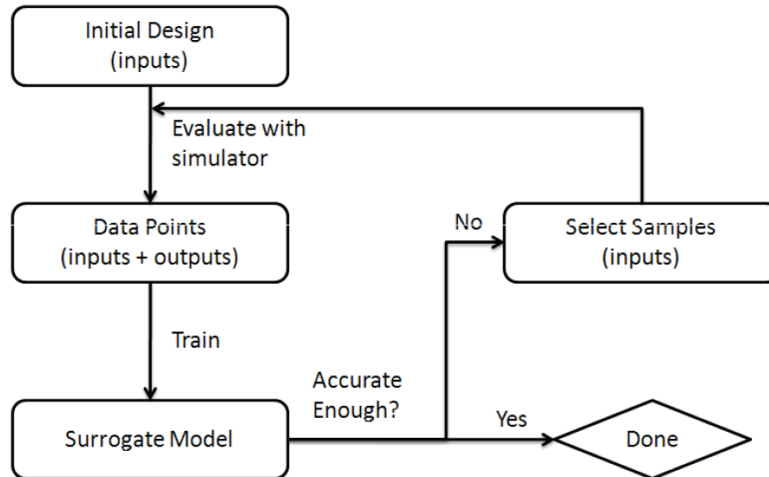


**FIGURE 4.** The workflow of a surrogate modeling routine for a certain system with input and output. Taken from the SUMO Toolbox Tutorial, Ivo Couckuyt, INTEC UGhent.

The technique that is employed to perform optimization is called surrogate modeling, for which we used the Matlab Surrogate Modeling (SUMO) Toolbox, developed by INTEC, UGhent [9]. This routine creates a model of a certain system for which we only know the input and output. The software achieves this by first choosing a set of initial input samples, based on a so called Latin Hypercube Design, and calculating the according output. It then builds a model through the resulting evaluated samples by use of the Kriging Modeling technique. From the obtained model the software chooses new samples to evaluate in order to improve the current surrogate model. The way these new samples are chosen is done by the Local Linear Adaptive Sampling Algorithm (LOLA), which identifies nonlinear regions in the current surrogate model to evaluate them more densely. A second routine, called the Dividing Rectangles Algorithm, determines the current minima of the model and evaluates them. This procedure is repeated until a certain tolerance is reached or when a maximum number of samples have been evaluated. The complete workflow is summarized on Fig. 4.

The parameters that are to be optimized still have to be chosen. After first manual sensitivity tests, the Young's moduli of the tympanic membrane and the extracolumella emerged as good candidates, since they influence the displacements of the eardrum more significantly than other parameters. The total object function of Eq. (1), and therefore also the resulting optimization, will be computed for the different applied sound frequencies separately, since viscoelastic parameters are known to be frequency dependent.

### 3. RESULTS

#### 3.1 Experimental Results

In order to interpret the results from digital holography, a temporal FFT-analysis is applied to the time-dependent displacement maps that are obtained from the experiments. From this analysis, vibration magnitude and phase relative to the sound signal at the TM are calculated for each object point. The results are presented in Fig. 5 as magnitude and phase maps for different stimulus frequencies. Fig. 6 shows the result from LDV measurements on the center of the columella footplate, as described in section 2.1. The figure presents footplate velocity amplitude as a function of input frequency. The sound pressure was kept at 90 dB SPL for all frequencies. The two distinct resonance peaks of roughly the same height are remarkable, as mammal middle ear transfer functions typically feature only one high resonance peak and multiple subsequent smaller peaks at higher frequencies.



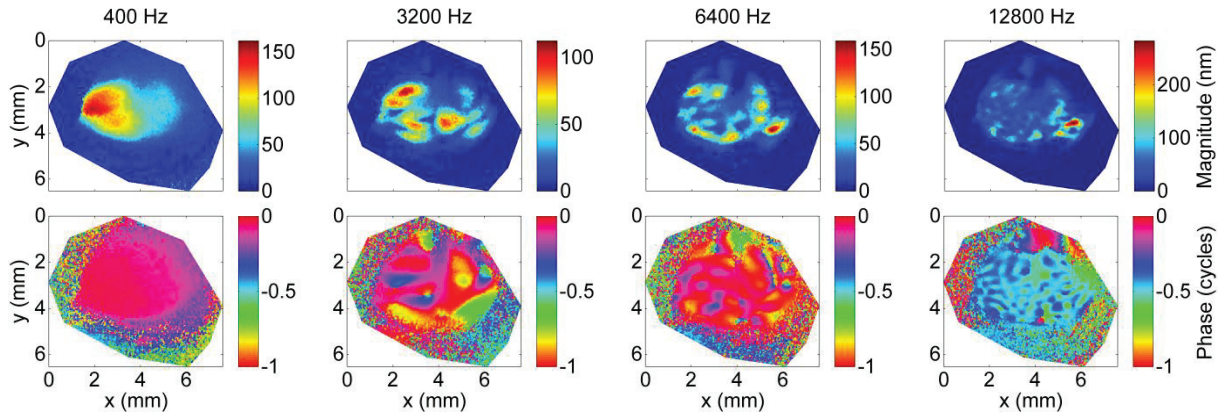


**FIGURE 5.** Displacement magnitude and phase maps of the duck eardrum, extracted from digital holography data at different frequencies.

### 3.2 Model results

This section contains preliminary results of the inverse analysis on the finite element model, based on holography measurements. A surrogate modeling routine was carried out on the object function between model and experiment as defined in Eq. (1), for which the Young's moduli of the eardrum and the extracolumella were incorporated as input parameters. The calculations were executed for the different applied sound frequencies separately, and results are shown for the example frequency of 1600 Hz in Fig. 7.

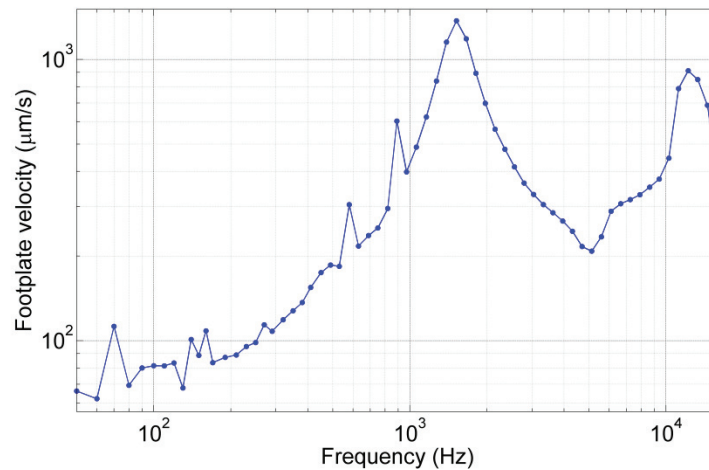


**FIGURE 6.** Velocity of the center point of the columella footplate, derived from LDV measurements. The sound pressure for all frequencies was kept at 90 dB SPL.

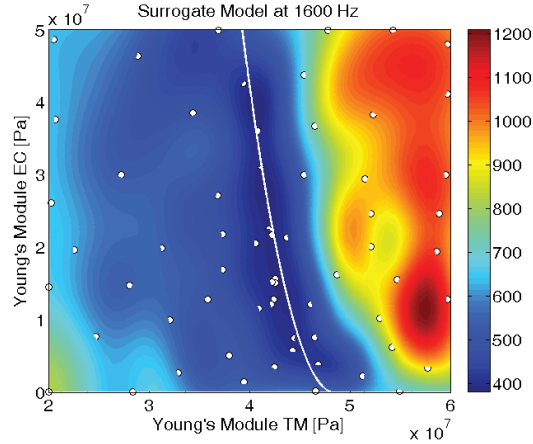


**FIGURE 7.** Inverse analysis on the Young's moduli of the tympanic membrane (TM) and the extracolumella (EC) at the sound frequency of 1600 Hz. The result is obtained by a surrogate modeling routine built with 64 samples. Colors on the plot represent the squared error between model and experiment, i.e. the object function as defined by Eq. (1).

The plots of the object function make clear that the eardrum Young's module  $E_{TM}$  has a bigger influence on the object function than the module of the extracolumella  $E_{EC}$ , which is not unexpected as we considered the eardrum displacements in our analysis. The optimal output values of the model lie on a curve inside a finite region of the input domain. To find this curve a fit was carried out using a second order polynomial with two parameters  $c_1$  and  $c_2$  by minimizing the line integral along the curve. The equation describing this polynomial is

$$E_{EC} = c_1(E_{TM} - c_2)^2. \tag{2}$$

The optimal values for the two parameters are  $[c_1, c_2] = [5,92 \cdot 10^{-7}, 4,85 \cdot 10^{-7}]$  at the chosen frequency. The minimum object function value along the fitted line was found at  $[E_{TM}, E_{EC}] = [40.3, 39.6]$  MPa for 1600 Hz. In Fig. 8 the displacement amplitude and phase of the tympanic membrane are compared for the holography measurements and the optimized finite element model. Note that results are preliminary as the study is still ongoing.

Although the results for the displacement patterns at these frequencies are more or less satisfactory, we would also like to obtain optimization results at lower frequencies, in which we might take the absolute displacements into account. Additionally we want to further reduce the range of possible Young's moduli we have optimized, especially for the extracolumella. The solution to this problem might be provided by the LDV measurements we performed on the footplate displacements. Moreover these experiments will give a better idea about how the avian middle ear deals with the transfer of sound energy from the outer to the inner ear. At the time of writing this manuscript, the LDV measurements have not yet been incorporated in the optimization of the model, but the combination of full-field holography data with high-resolution LDV results is a promising approach for validation and optimization of the model.

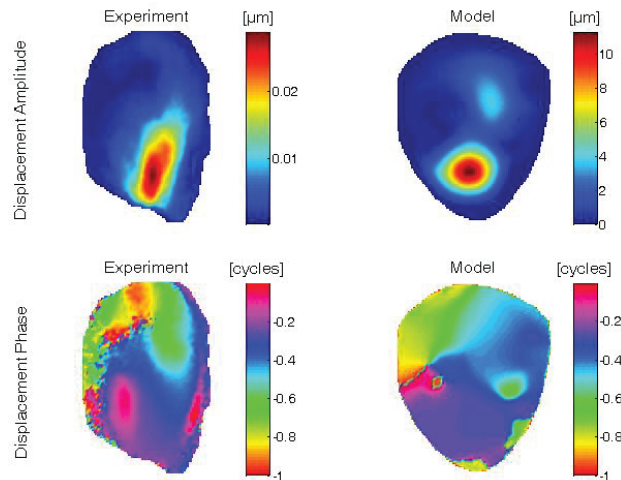


**FIGURE 8.** The displacement amplitude and phase of the tympanic membrane, compared for the results of the holography measurements and optimized finite element model. Notice that the inverse analysis was obtained only by considering the normalized displacement patterns, in contrast to the absolute displacements.



## 4. CONCLUSION

In order to investigate the mechanics of complex biomechanical systems such as the avian middle ear, we believe that a multidisciplinary approach is necessary. Therefore, a combination of optical experiments and computerized finite element modeling has been used in this work. Experiments consisted of digital stroboscopic holography measurements on an acoustically stimulated duck eardrum at different separate frequencies, which provided full-field time-resolved displacement maps. These full-field data were complemented by single-point velocity data from LDV measurements on the columella footplate, which is the final structure of the avian middle ear. The combination of these experiments provides valuable data on the role of the avian middle ear as an impedance match between the outer and inner ear and results of both are presented in this paper.

Based on contrast-enhanced high-resolution  $\mu$ CT measurements, a finite element model of the duck middle ear was constructed. Using the experimental holography data, different influential parameters have been optimized to minimize an object function between experimental and model outcome. The parameters that were chosen to be optimized are the Young's moduli of the TM and the extracolumella. The object function was found to be minimal for values for these parameters of 40.3 MPa (TM) and 39.6 MPa (EC) at 1600 Hz. These were found through an inverse analysis routine, based on the Matlab Surrogate Modeling (SUMO) Toolbox (INTEC, UGhent), as explained in detail. The presented values are based on only the holography results, since the LDV results were not incorporated in the optimization at the time of writing.

## ACKNOWLEDGMENTS

This work was financially supported by the Research Foundation Flanders (FWO) and the University of Antwerp.

## REFERENCES

1. R. Dooling, "Avian Hearing and the Avoidance of Wind Turbines Avian Hearing and the Avoidance of Wind Turbines" (Colorado, 2002), p. 84.
2. D. De Greef, J. J. J. Dirckx, "Measurement of Rabbit Eardrum Vibration through Stroboscopic Digital Holography", AIP Proceedings, this issue (2014)
3. B.C. Masschaele, V. Cnudde, M. Dierick, P. Jacobs, L. Van Hoorebeke, and J. Vlassenbroeck, Nucl. Instruments Methods Phys. Res. Sect. A Accel. Spectrometers, Detect. Assoc. Equip. 580, 266 (2007).
4. D. De Greef, J. Aernouts, J. Aerts, J.T. Cheng, R. Horwitz, J.J. Rosowski, and J.J.J. Dirckx, "Viscoelastic properties of the human tympanic membrane studied with stroboscopic holography and finite element modeling," Hear. Res. (2014). (submitted, DOI: 10.1016/j.heares.2014.03.002)
5. K. Homma, Y. Shimizu, N. Kim, Y. Du, and S. Puria, Hear. Res. 263, 204 (2010).
6. G. Spahn and R. Wittig, Zentralbl. Chir. 128, 78 (2003).
7. K. Homma, Y. Du, Y. Shimizu, and S. Puria, J. Acoust. Soc. Am. 125, 968 (2009).
8. H. Cai, R.P. Jackson, C.R. Steele, and S. Puria, in Proc. COMSOL Conf. (2010).
9. D. Gorissen and T. Dhaene, J. Mach. Learn. Res. 11, 2051 (2010).